AGU PUBLICATIONS

Geochemistry, Geophysics, Geosystems

TECHNICAL REPORTS: DATA

10.1002/2016GC006401

Key Points:
- First margin-wide total sediment thickness grid, with observed thickness up to 4 km
- Preglacial, transitional, and full glacial sequences across several studies linked and gridded
- Distinct eastward shift of depocenters near the Eocene/Oligocene transition

Supporting Information:
- Table S1
- Table S2

Correspondence to:
A. Lindeque,
ansa.lindeque@icloud.com

Citation:
Lindeque, A., K. Gohl, F. Wobbe, and G. Uenzelmann-Neben (2016), Preglacial to glacial sediment thickness grids for the Southern Pacific Margin of West Antarctica, *Geochem. Geophys. Geosyst.*, *17*, 4276–4285, doi:10.1002/2016GC006401.

Received 12 APR 2016
Accepted 16 SEP 2016
Accepted article online 3 OCT 2016
Published online 28 OCT 2016

Preglacial to glacial sediment thickness grids for the Southern Pacific Margin of West Antarctica

Ansa Lindeque[1], Karsten Gohl[1], Florian Wobbe[1], and Gabriele Uenzelmann-Neben[1]

[1]Alfred-Wegener-Institut Helmholtz-Zentrum für Polar- und Meeresforschung, Bremerhaven, Germany

Abstract Circum-Antarctic sediment thickness grids provide constraints for basin evolution and paleotopographic reconstructions, which are important for paleo-ice sheet formation histories. By compiling old and new seismic data, we identify sequences representing preglacial, transitional, and full glacial deposition processes along the Pacific margin of West Antarctica. The preglacial sediment grid depicts 1.3–4.0 km thick depocenters, relatively evenly distributed along the margin. The depocenters change markedly in the transitional phase at, or after, the Eocene/Oligocene boundary when the first major ice sheets reached the shelf. Full glacial sequences, starting in the middle Miocene, indicate new depocenter formation North of the Amundsen Sea Embayment and localized eastward shifts in the Bellingshausen Sea and Antarctic Peninsula basins. Using present-day drainage paths and source areas on the continent, our calculations indicate that an estimated observed total sedimentary volume of $\sim 10 \times 10^6$ km^3 was eroded from West Antarctica since the separation of New Zealand in the Late Cretaceous. Of this, 4.9×10^6 km^3 predates the onset of glaciation and need to be considered for a 34 Ma paleotopography reconstruction. Whereas 5.1×10^6 km^3 postdates the onset of glaciation, of which 2.5×10^6 km^3 were deposited in post mid-Miocene full glacial conditions.

1. Introduction

Sediment thickness grids provide important constraints for basin evolution as well as reconstructing paleobathymetric and paleotopographic models. Such paleotopographic reconstructions of Antarctica play a particular role in explaining processes of paleo-ice sheet formation and dynamics [e.g., *Wilson et al*., 2012, 2013]. The preglacial to glacial sequences in the polar marine sedimentary record document the changeover from greenhouse to icehouse climate conditions and provide indications of the ice sheet extent in times of important climatic changes [e.g., *Anderson and Bartek*, 1992; *Brancolini et al*., 1995; *Rebesco et al*., 1997; *De Santis et al*., 2003; *DeConto and Pollard*, 2003; *Wilson and Luyendyk*, 2009; *Brancolini and Leitchenkov*, 2010]. Based on various seismostratigraphy studies around the Antarctic margin, the marine sedimentary column can be generally subdivided into the "preglacial," the "transitional," and the "full glacial" sequences [e.g., *Lindeque et al*., 2013, 2016; *Huang et al*., 2014], spanning approximately 90 Myr of basin evolution history [*Wobbe et al*., 2012, 2014; *Lindeque et al*., 2016]. The transitional sequence includes sediments deposited from the onset of major early ice sheet development near the Eocene-Oligocene (E/O) boundary at about 34 Ma. In the Oligocene to the middle Miocene, at about 15 Ma, ice sheet advances to and across the continental shelves intensified with transport and deposition of sediments, forming the full glacial sequence.

By mapping the seismic boundary horizons of these sequences, regions of high sediment deposition, referred to as depocenters, can be identified. Although these depocenters hold minor proportions of pelagic and hemipelagic components, the sources mainly point to alluvial and glacial drainage outlets from the continent. Relocations of such depocenters in particular time periods document changes in sediment transport due to bottom current development, which can be associated with changes in climate and glacial conditions.

The seismic data used to generate reasonable isopach maps have been unevenly distributed around Antarctica. *Whittaker et al*. [2013] and *Wobbe et al*. [2014] published improved total sediment thickness grids of the southeastern Indian Ocean between Australia and East Antarctica, and off the Pacific margin of West Antarctica, respectively. A recent compilation of seismic data enabled the generation of a regional

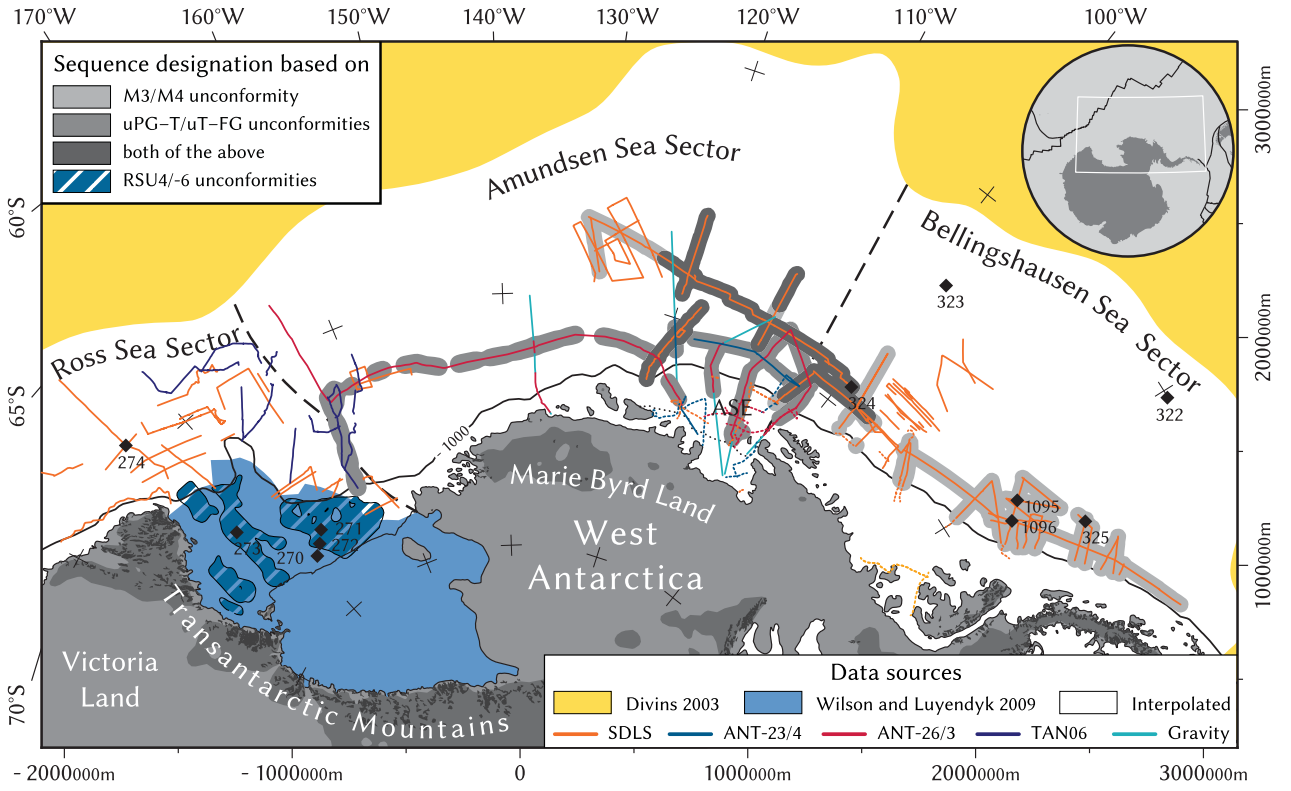

Figure 1. Source identification map modified after *Wobbe et al*. [2014]. Total sediment thickness model is based on data from *Divins* [2003, yellow area], *Wilson and Luyendyk* [2009, light blue area], interpretations of seismic data (thin lines), and DSDP borehole information (black diamonds). Thin dashed lines mark seismic lines on the Amundsen and Bellingshausen Sea shelves that either do not record major sediments on top of basement (inner shelves) or do not record top of basement. These lines were not used for the sediment thickness grids. Intermediate white area is interpolated. uPG-T/uT-FG unconformities interpreted from selected seismic profiles (gray-shaded buffers around lines) and *ANTOSTRAT* [1995, blue striated area].

seismostratigraphy, sediment thickness grids and paleobathymetric models of the Weddell Sea basin [*Lindeque et al*., 2013; *Huang et al*., 2014]. The Ross Sea shelf (Figure 1) has the highest coverage of seismic data, which *Wilson and Luyendyk* [2009] used to publish an initial 34 Ma topography of West Antarctica, incorporating the sediment thickness of units above the E/O unconformity, RSU6. However, the Ross Sea sediment thickness grids stand in isolation from earlier isopach grids of the Bellingshausen Sea [*Scheuer et al*., 2006], due to a lack of seismic data needed to link the sequence horizons across the Amundsen Sea (Figure 1). In addition, the Bellingshausen Sea grids only identified sediments for the full glacial period (mid-Miocene, ~10 Ma onward), but the E/O boundary remained unidentified. New seismic data acquisition in the previously unexplored western and central Amundsen Sea (Figure 1) [*Gohl*, 2010; *Lindeque et al*., 2016] and the integration of existing sedimentary thickness grids for the eastern Amundsen Sea [*Scheuer et al*., 2006; *Uenzelmann-Neben and Gohl*, 2012, 2014], allow us to correlate a first margin-wide seismic stratigraphy and construct preglacial, transitional, and full glacial isopach grids for the southern Pacific margin of West Antarctica.

2. Database and Methods

We largely improve the total sediment thickness grid for the Pacific margin of West Antarctica [*Wobbe et al*., 2014] by identifying the top of basement from recently acquired multichannel seismic data in the eastern Ross Sea (TAN0602 survey in *Lindeque et al*. [2016]) and western to central Amundsen Sea (ANT-2010 survey in *Lindeque et al*. [2016]). Having this as a base data set (Figure 1, produced in polar stereographic projection referenced to WGS84 with true scale latitude at 71°S and central meridian at 138°W), we construct new basin-wide preglacial, transitional, and full glacial sediment thickness grids of 5 km cell size, using the correlated E/O boundary (34 Ma) and mid-Miocene (15 Ma) horizons from published seismic data and borehole information of the Ross Sea, Amundsen Sea, and Bellingshausen Sea basins. An overview of the source

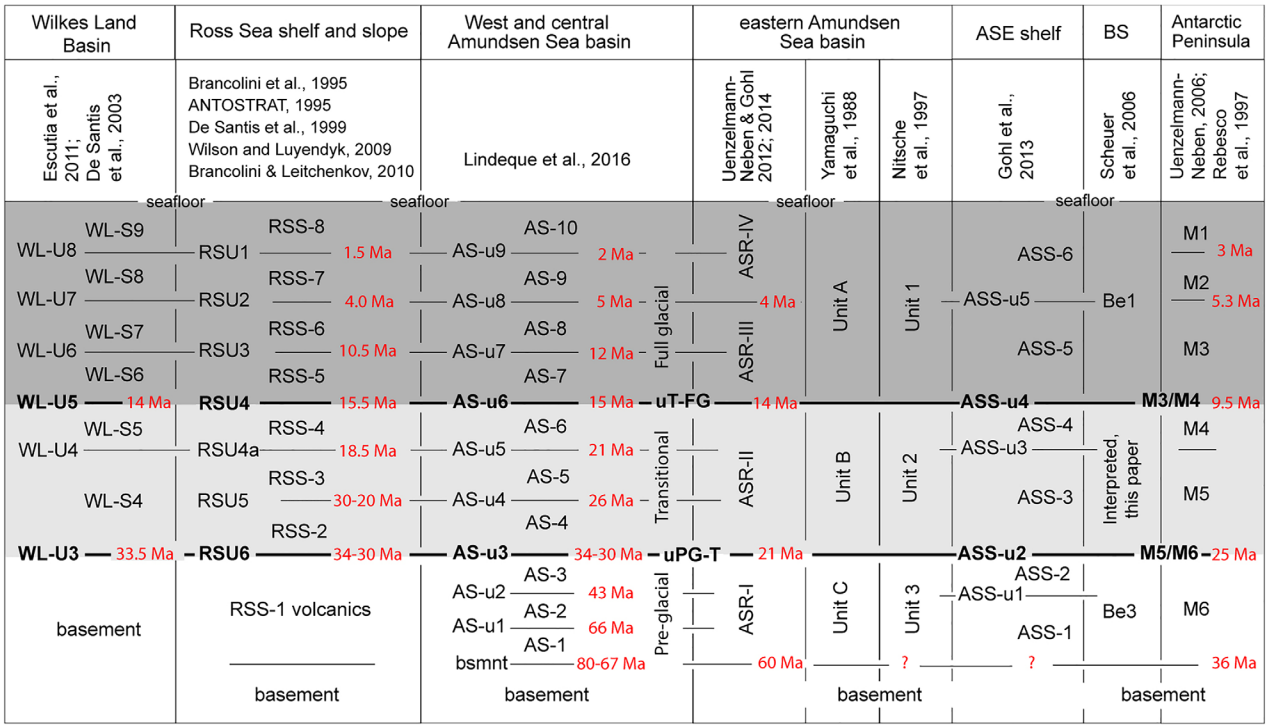

Figure 2. Seismic stratigraphic correlation chart of seismic interpretations along the Pacific margin of West Antarctica with published ages of key horizons.

identification and the seismic profiles used in the grid constructions are listed in supporting information Table S1.

2.1. Stratigraphic Correlation

The margin-wide seismic horizon correlation is summarized in Figure 2. Supporting age control from boreholes (Figure 1) is drawn from IODP Leg 318 Site U1356 off Wilkes Land [*Escutia et al.*, 2011], DSDP Leg 28 Sites 270–274 in the Ross Sea [*Hayes and Frakes*, 1975], DSDP Leg 35 Sites 322–324 in the Bellingshausen Sea [*Hollister et al.*, 1976; *Tucholke et al.*, 1976], and ODP Leg 178 Sites 1095 and 1096 off the central Antarctic Peninsula [*Rebesco et al.*, 1997; *Barker et al.*, 2002; *Uenzelmann-Neben*, 2006].

The Ross Sea shelf and slope seismic stratigraphy are used as published (Figure 2). *Lindeque et al.* [2016] correlated the new data of the western and central Amundsen Sea basin to the interpreted sequences of the Wilkes Land margin by linking the seismic horizons via the known Ross Sea shelf stratigraphy [*Anderson and Bartek*, 1992; *ANTOSTRAT*, 1995; *Brancolini et al.*, 1995; *De Santis et al.*, 1999, 2003; *Wilson and Luyendyk*, 2009; *Brancolini and Leitchenkov*, 2010].

To the east, the sedimentary sequences of the central Amundsen Sea basin are correlated to the seismic stratigraphy of the eastern Amundsen Sea and Bellingshausen Sea [*Yamaguchi et al.*, 1988; *Nitsche et al.*, 1997, 2000; *Rebesco et al.*, 1997; *Scheuer et al.*, 2006; *Uenzelmann-Neben*, 2006; *Uenzelmann-Neben and Gohl*, 2012, 2014; *Gohl et al.*, 2013]. We expand on the correlation by *Lindeque et al.* [2016] and trace their two key regional seismic horizons, the uPG-T being close to the E/O transition and mid-Miocene uT-FG, to the horizon interpretation of the eastern Amundsen Sea basin, Bellingshausen Sea, and Antarctic Peninsula (Figure 2). The seismic horizon picks of *Scheuer et al.* [2006] and *Rebesco et al.* [1997] were used as published. The only change is that the seismic lines in the isopach grids of *Scheuer et al.* [2006] did not identify a horizon near the E/O transition; we added this to the seismic lines they used.

2.2. Sediment Thickness Calculation

We expanded the total sediment thickness grid of *Wobbe et al.* [2014], shown in Figure 3, and derived three sediment unit thickness grids: (i) The preglacial (PG) sequence (Figure 4) representing the sediments

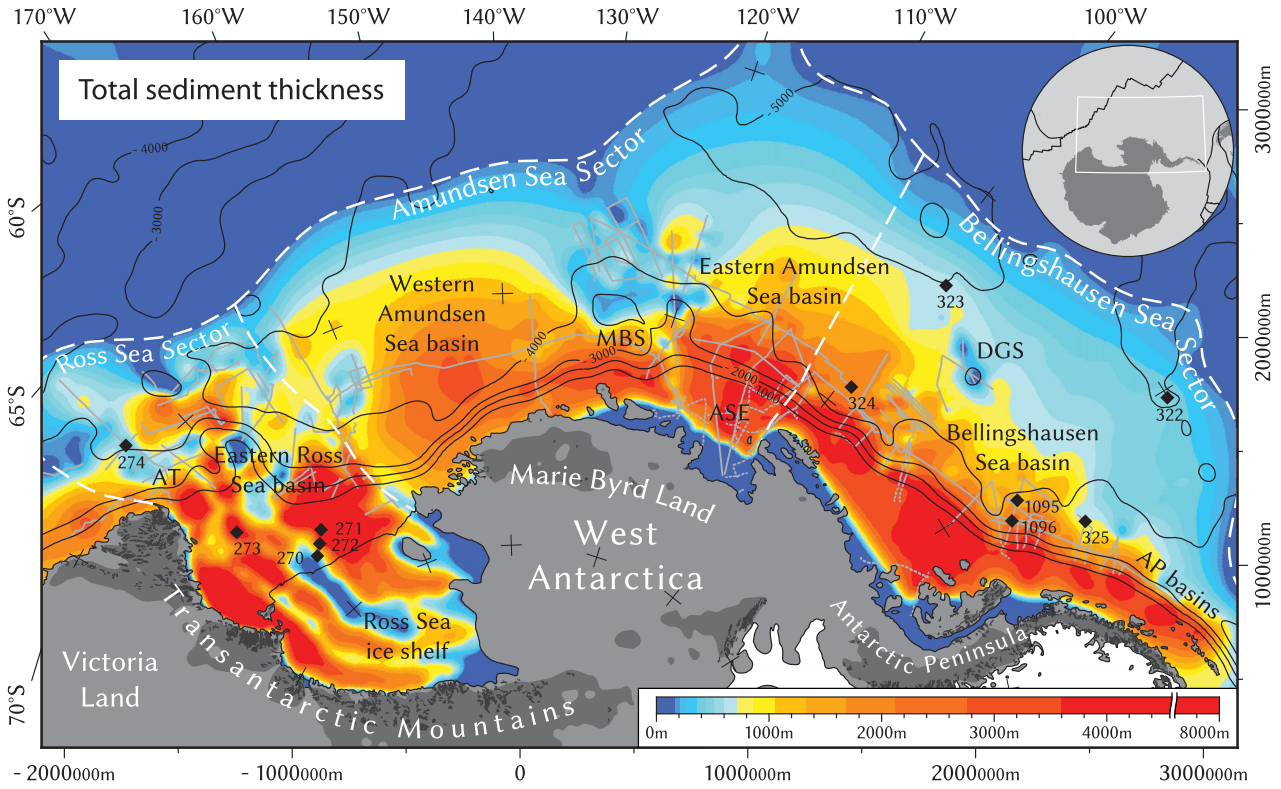

Figure 3. Total observed sediment thickness grid along the Pacific margin of West Antarctica, modified after *Wobbe et al*. [2014]. White dashed lines mark the sector boundaries. Gray lines show published seismic reflection data used for the seismic horizon stratigraphy correlation and construction of subsequent grids of Figures 3–5. Black diamonds indicate DSDP and ODP drill sites used for stratigraphic and chronological control. Dark grey areas illustrate Ross Sea regions with a present-day bathymetry above 500 m. Abbreviations are: MBS—Marie Byrd Seamounts, ASE—Amundsen Sea Embayment, AP—Antarctic Peninsula, DGS—De Gerlache Seamounts. Map is produced in polar stereographic projection referenced to WGS84 with true scale latitude at 71°S and central meridian at 138°W.

deposited before the built-up of major ice sheets that extended to the coastal zone and the shelf. The sequence is estimated to be of Oligocene-Eocene age or older [*Lindeque et al*., 2013, 2016], and bounded by the acoustic basement below and the uPG-T horizon above. (ii) The transitional (T) sequence (Figure 5), which consists of Oligocene to middle Miocene sediments associated with the first arrival of the major ice sheets at the coasts and shelves. The sequence is bounded by the mid-Miocene uT-FG horizon above. (iii) The full glacial (FG) sequence (Figure 6) above horizon uT-FG, consists of sediments associated with pronounced advances of grounded ice across the shelves.

We convert the two-way-travel times (TWT, T in s) for each boundary horizon to depth Z (km) using the empirical time-depth relation $Z = 3.03 \ln(1 - 0.52T)$ of *Carlson et al*. [1986] for the top sediments of less than 1.4 s TWT (~1.4 km thick). For deeper sediments, the *P*-wave velocities from the sparse seismic refraction measurements of the Pacific margin of West Antarctic are considered. Sonobuoy data of the eastern Ross Sea rise recorded interval velocities from 1600 to 3900 m/s (TAN0602 survey in *Lindeque et al*. [2016]). These compare well with the velocities from the *P*-wave refraction velocities of the sediments in the eastern Amundsen Sea, which range from 1600 to 4200 m/s [*Gohl et al*., 2007; *Kalberg and Gohl*, 2014]. Interval velocities derived from stacking velocities of the multichannel seismic data in the central Amundsen Sea range from 1690 to 3760 m/s down to a maximum sediment depth of 3.9 km below seafloor [*Lindeque et al*., 2016] and are consistent with the velocities of the seismic refraction data. Sediments deeper than 2.8 s TWT were converted to depth using an average interval velocity of 2820 m/s.

2.3. Data Merging and Gridding

We use the same approach as in *Wobbe et al*. [2014] in order to maintain consistency for comparison of previous sediment thickness grids available at the National Geophysical Data Center [NGDC] and PANGAEA. 10 × 10 km block medians were calculated to avoid spatial aliasing and short-wavelength artifacts in the

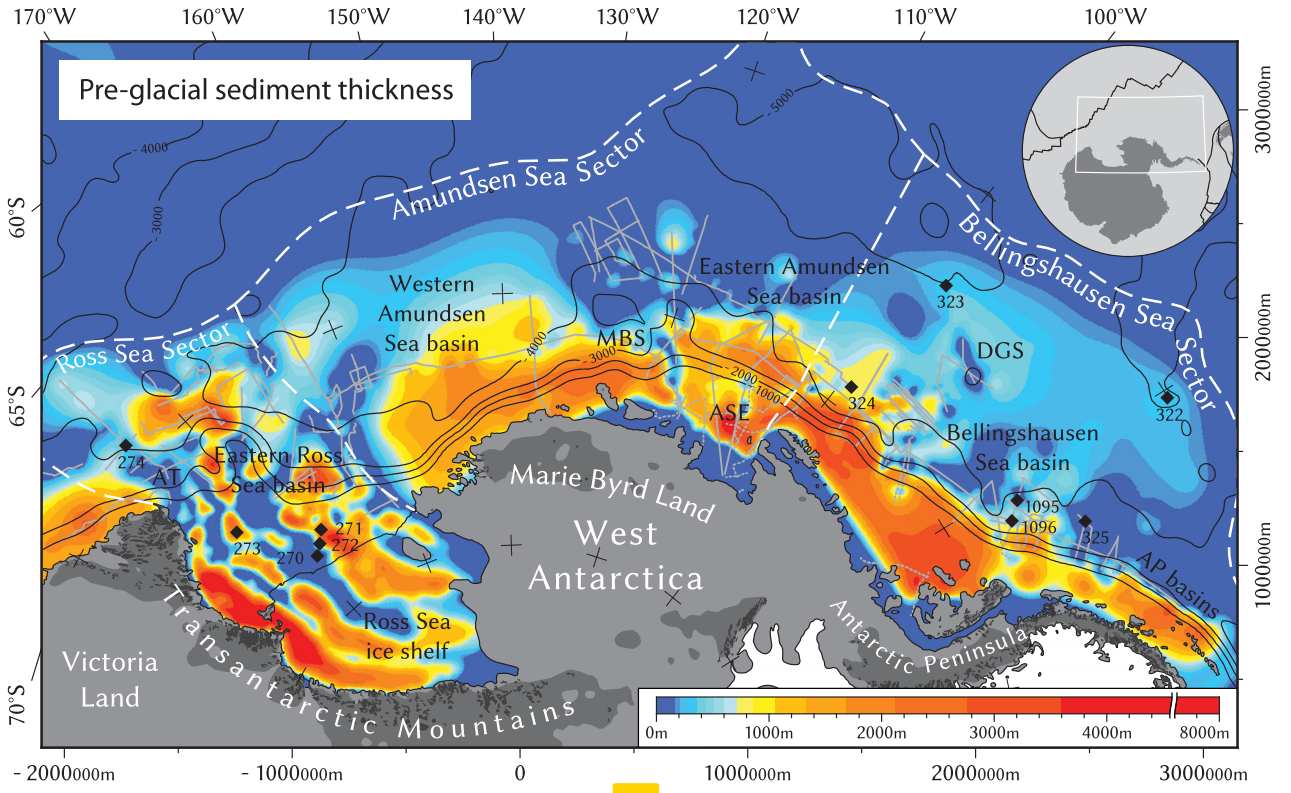

Figure 4. The preglacial sediment thickness grid, including all units up to the uP[illegible]oundary of Figure 2. Annotations and map projection are the same as in Figure 1.

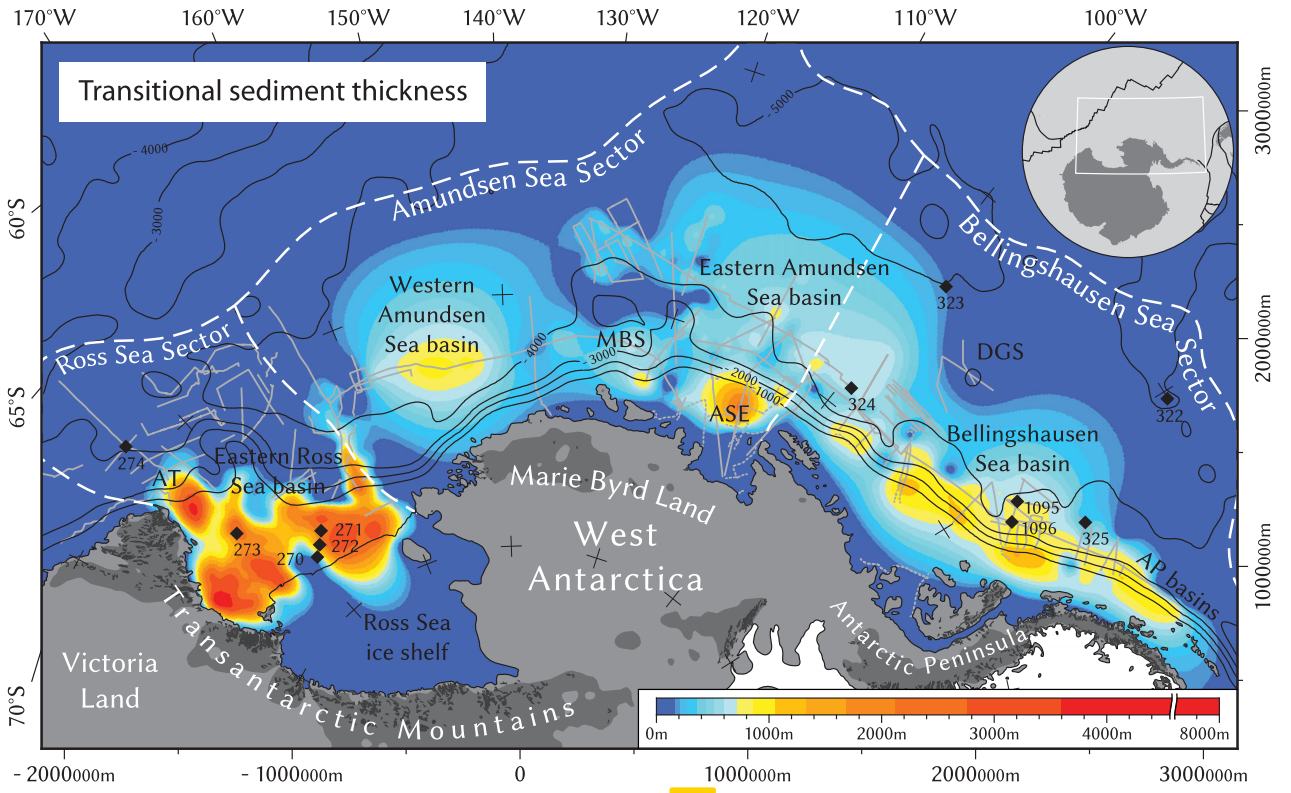

Figure 5. The transitional sediment thickness grid, including all seismic units between the uPG-T[illegible]he uT-FG boundary of Figure 2. Annotations and map projection are the same as in Figure 1.

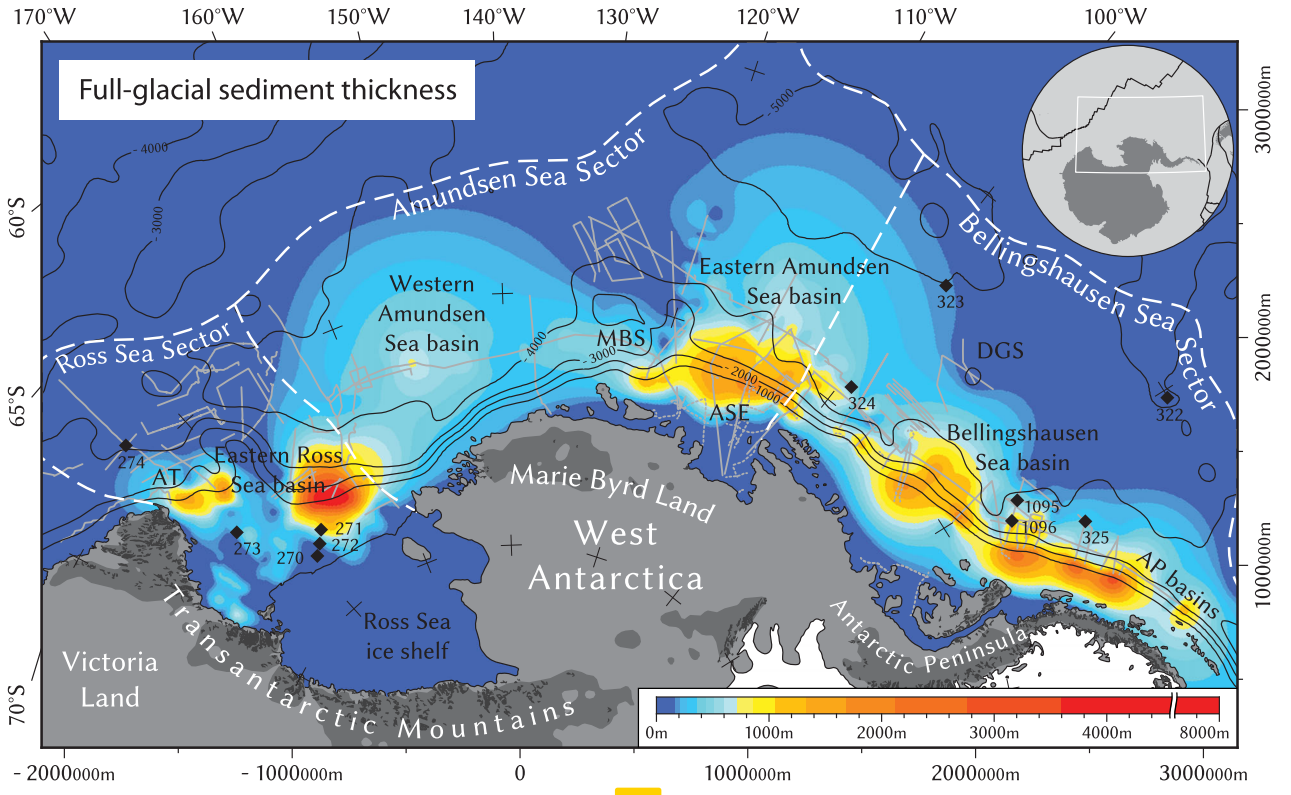

Figure 6. The full glacial sediment thickness grid, including all seismic units above th G boundary of Figure 2. Annotations and map projection are the same as in Figure 1.

gridding process. Local minima and maxima were suppressed by applying a 0.2 tension factor to the continuous curvature splines gridding algorithm of *Smith and Wessel* [1990].

To avoid distortions and still maintain reasonable appearance of the PG, T, and FG grids, outliers were manually identified and excluded in areas devoid of seismic data. This was especially the case on unmapped shelves. A second-order Butterworth low-pass filter with a cutoff wavelength of 100 km was applied to remove short-range variations. A variable area correction of the grid was not applied because the distortion of the Conformal versus Equal Area approach does not exceed 5% in the region of interest and is considered negligible at this scale. The final grids were resampled by bicubic interpolation to 5 km resolution.

We divided the West Antarctic margin into three main deposition sectors (Figure 1) according to the terrigenous sediment source areas determined from the present-day ice drainage system divides [*Zwally et al.*, 2012]. The Ross Sea sector covers an area of 1.76×10^6 km^2, the Amundsen Sea sector 3.43×10^6 km^2, and the Bellingshausen Sea sector 2.91×10^6 km^2. Table 1 summarizes the observed sedimentary volumes of the PG, T, and FG sequences in the three sectors, and the hypothetical volume of sediment that would cover West Antarctica if the sediments were restored back to their source areas. Mean observed sediment thicknesses for each unit are listed in supporting information Table S2. We applied *Wilson et al.*'s [2012]

Table 1. Observed Sedimentary Volumes (in 10^6 km^3) and Volume Fractions (in %) of the Preglacial (PG), Transitional (*T*), and Full Glacial (FG) Sequences in the Ross Sea (RS), Amundsen Sea (AS), and Bellingshausen Sea (BS) Sectors[a]

		RS	AS	BS	All
Volume	FG	0.44 (16%)	1.05 (29%)	1.03 (28%)	2.51 (25%)
	T	0.82 (29%)	0.91 (25%)	0.85 (23%)	2.58 (26%)
	PG	1.52 (55%)	1.60 (45%)	1.73 (48%)	4.86 (49%)
	Total	2.78	3.56	3.61	9.95
Area	Total	1.76	3.43	2.91	8.10

[a]The total area of each of these three each sectors (in 10^6 km^2) is listed in the bottom row and corresponding column.

estimates for in situ sediment density (1.95–2.1 g/cm^3) and source rock density (2.6 g/cm^3), a maximum pelagic fraction of 15% were considered, but not restored to the continent in this calculation.

3. Results and Discussion

3.1. Reliability and Uncertainties of the Grids

In general, our isopach grids represent approximate time intervals in which certain sedimentation processes were dominant. Due to the lack of sufficient deep drilling sites along the West Antarctic margin and southern Pacific, the stratigraphic age model is prone to large uncertainties, which is demonstrated by lateral variations in the ages associated to our horizons. For instance, we assigned an age of around 34–30 Ma for the dominant uPG-T horizon in the Ross Sea and western Amundsen Sea rise, but younger ages (25–21 Ma) for the same horizon in the eastern Amundsen Sea and Bellingshausen Sea basins [*Lindeque et al*., 2016].

Additional uncertainties stem from the sparse data point distribution in some areas due to limited seismic data. It is likely that sediments are thicker than estimated in some continental shelf and slope areas, where the preglacial to glacial units could not be identified. The transitional and full glacial units on the continental rise of the Ross Sea are currently underestimated because others are still working at the seismostratigraphic analysis of a large number of seismic lines. In a broad assumption, the preglacial volume may be uncertain by ±30% while the younger volumes may be uncertain by ±20% due to limited mapping, boreholes, and seismic data distributions.

It can be assumed that the three sedimentary units consist mostly of terrigeneous sediments with minor proportions of pelagic and hemipelagic components. DSDP and ODP boreholes revealed about 15% of pelagic components in their cores, but it is uncertain whether this proportion is representative for the entire continental rise from the Ross Sea to the Bellingshausen Sea.

We are confident that our time-depth conversion yields relatively realistic thickness values, because of seismic refraction and sonobuoy velocities from the Amundsen Sea and the Ross Sea, respectively, showing similar velocity-depth distribution.

3.2. Preglacial Sediment Thickness Grid

The preglacial sequence depicts depocenters that are relatively evenly distributed along the West Antarctic continental rise, ranging in maximum thickness from 1.3 km in the western Amundsen Sea to more than 4 km in the Ross Sea and eastern Bellingshausen Sea (Figure 4). The thickest depocenters are in the eastern Ross Sea and eastern Amundsen Sea. The oldest sediments of this sequence were deposited on the oldest oceanic crust, determined from magnetic seafloor spreading anomalies used for plate-kinematic reconstructions [e.g., *Eagles et al*., 2004; *Wobbe et al*., 2012]. This oldest crust ranges from 90 Ma south of magnetic spreading anomaly C34 in the eastern Amundsen Sea, to about 84–79 Ma on the western Amundsen Sea and Ross Sea rise, and to less than 40 Ma west of the Antarctic Peninsula. From the margin-wide stratigraphic correlation (Figure 2), the youngest limit of this sedimentary unit ranges from about 34 Ma in the western Amundsen Sea to 21 Ma in the eastern Amundsen Sea. Refer to *Wobbe et al*. [2012] for a detailed account of the Amundsen Sea basin evolution and geodynamics along the margin.

The fairly even distribution of deposition is interpreted as sediment supply coming from most of the continental regions. The Ross Sea sediment thickness distribution was likely controlled by the tectonic evolution of the rift basins [*Davey*, 1987], with the Terror Basin and the Eastern Basin being the prominent depocenters throughout the Tertiary rifting phase [*Cooper et al*., 1991]. A shift in depocenters from the Bellingshausen Sea to the Antarctic Peninsula reflects the uplift and subsidence processes associated with the south to north ridge-trench collision [*Anderson*, 1999].

This period has the highest sediment volume across all areas (Table 1). The reconstructed West Antarctic paleotopography at 34 Ma by *Wilson and Luyendyk* [2009] and *Wilson et al*. [2012] shows a landmass of West Antarctica with a higher average elevation than today, and it is reasonable to assume that a high erosion rate contributed to the large and wider distributed sediment supply along the margin.

3.3. Transitional Sediment Thickness Grid

The up to 1.8 km thick transitional sequence (Figure 5) shows a clear concentration of depocenters in the eastern Ross Sea, the western Amundsen Sea as well as the Bellingshausen Sea and Antarctic Peninsula

basins. Our stratigraphic correlation (Figure 2) along the margin places an estimated maximum age range from 34 to 10 Ma on this sequence. We relate this time interval to sedimentation processes affected by increasing continental ice sheets that expanded to the coasts and inner shelves [e.g., *Anderson and Bartek*, 1992; *Lear et al*., 2008; *Miller et al*., 2008; *Wilson et al*., 2013; *Gohl et al*., 2013] as the global temperatures generally decreased [e.g., *Zachos et al*., 2001, 2008].

We speculate that increased bottom-water circulation caused by perennial sea-ice cover, may have transported large volumes of sediment in an eastward direction [*Uenzelmann-Neben and Gohl*, 2012, 2014] and, thus, forced the formation of localized depocenters. Fast erosion by first major ice sheets likely altered the topography of West Antarctica [*Wilson et al*., 2012, 2013]. Ice flow drainage may have been redirected and became more concentrated to follow major drainage pathways along eroded lowered topography, possibly following tectonic displacement zones such as faults or rifts zones associated with the West Antarctic Rift System [*Davey and De Santis*, 2006; *Müller et al*., 2007; *Wilson and Luyendyk*, 2009; *Gohl et al*., 2013]. Such processes would account for the concentration of glacial deposits in the eastern Ross Sea, western Amundsen Sea and Bellingshausen Sea.

The relatively high sediment supply to the Bellingshausen Sea can also be associated with the subduction orogeny of the central and northern part of the Antarctic Peninsula, which was still active in this time interval.

3.4. Full Glacial Sediment Thickness Grid

The full glacial sequence (Figure 5) represents the Antarctic-wide time interval from the mid-Miocene (15 to 10 Ma) with dominant sedimentary deposits associated with ice sheets advancing across the shelves more frequently in glacial periods [e.g., *Rebesco et al*., 1997; *Nitsche et al*., 1997, 2000; *De Santis et al*., 1999, 2003; *Uenzelmann-Neben*, 2006; *Smith and Anderson*, 2010, 2011; *Uenzelmann-Neben and Gohl*, 2012, 2014; *Gohl et al*., 2013; *Lindeque et al*., 2016]. Sediment supply increased compared to the transitional period (Table 1). The full glacial sequence indicates a change in depocenter locations along the margin (Figure 5). The western Amundsen Sea received less sediment input, while a new depocenter of up to 2 km thickness formed North of the Amundsen Sea Embayment (ASE). Such lateral variation could be due to uplift or denudation of the source area, but much of the sediment supply of the ASE can also be associated with the further development of ice streams draining from the catchment areas of the Pine Island and Thwaites Glacier systems [e.g., *Bamber et al*., 2009; *Gohl et al*., 2013; *Uenzelmann-Neben and Gohl*, 2014].

Deposition of the Bellingshausen Sea basin seems to have increased since the transitional period, probably in response to a growing Antarctic Peninsula Ice Sheet frequently grounded on the shelf [*Rebesco et al*., 1997; *Uenzelmann-Neben*, 2006]. Much of the Antarctic Peninsula remained at high elevation with erosional rates and sediment supply remaining high [*Lindeque et al*., 2013].

The combined T and FG volumes for the Ross Sea (1.26×10^6 km^3; Table 1), Amundsen Sea (1.96×10^6 km^3) and Bellingshausen Sea (1.88×10^6 km^3), from 50 to 160°W, are well within the range given in *Wilson and Luyendyk* [2009] and *Wilson et al*. [2012]. The mean observed sediment thickness estimates (supporting information Table S2) also compare well with previous work

4. Conclusions

Recently acquired seismic data in the central and western Amundsen Sea and eastern Ross Sea now allow basin-wide seismic stratigraphic correlation from the Ross Sea to the Bellingshausen Sea. From this correlation and the few available borehole data, we present sediment thickness grids for the total sedimentary cover as well as the preglacial (from <34 Ma), transitional (from >34 Ma to <15 Ma), and full glacial (from >15 Ma to present) sequences. The total sediment thickness grid updates the global NGDC grid for the southern Pacific sector. In total, an average of ~4.6 km thickness of the West Antarctic landmass was eroded and deposited as a total sedimentary volume of $\sim 10 \times 10^6$ km^3 along the Pacific margin from the Cretaceous to present day.

The preglacial period shows a fairly equal distribution of deposits along the entire West Antarctic margin, but the marker horizon uPG-T denotes the change of deposition pattern at the beginning of the transitional period after the first built-up of major ice sheets extending to the coasts and inner shelves. Depocenters

developed in the eastern Ross Sea, western Amundsen Sea, and Bellingshausen Sea. After ice sheets advances became more frequent, with grounding across the shelves beginning in the mid-Miocene as marked with the marker horizon uT-FG, the western Amundsen Sea basin was no longer a main depocenter, and a new depocenter developed north of the Amundsen Sea Embayment.

Acknowledgments

This project was funded by the Priority Program 1158 *Antarctic Research* of the *Deutsche Forschungsgemeinschaft* [DFG] under project number GO 724/10-1 and by institutional funds for Work Package 3.2 of the AWI Research Program PACES-II. This project contributes to the Scientific Research Project *Past Antarctic Ice Sheet Dynamics* (PAIS) of the *Scientific Committee on Antarctic Research* (SCAR). Seismic data other than those acquired by the AWI (AWI-xx) and GNS Science (TAN06xx) were obtained with thanks from the *Antarctic Seismic Data Library System* (SDLS; http://sdls.ogs.trieste.it). All isopach grids and maps were created using *Generic Mapping Tools* (GMT) Version 5 [*Wessel et al.*, 2013]. The data used are listed in the references and in the supporting information. The grid data sets are available from the Pangaea.de repository at URL/DOI https://doi.pangaea.de/10.1594/PANGAEA.864906. The authors wish to thank Doug Wilson and John Anderson for constructive reviews, which improved the manuscript.

References

Anderson, J. B. (1999), *Antarctic Marine Geology*, 289 pp., Cambridge Univ. Press, Cambridge, U. K.

Anderson, J. B., and L. R. Bartek (1992), Cenozoic glacial history of the Ross Sea revealed by intermediate resolution seismic reflection data combined with drill site information, in *The Antarctic Paleoenvironment: A Perspective on Global Change, Part One, Ant. Res. Ser.*, vol. 56, edited by J. P. Kennett and D. A. Warnke, pp. 231–263, AGU, Washington, D. C.

ANTOSTRAT (1995), Seismic stratigraphic Atlas of the Ross Sea, in *Geology and Seismic Stratigraphy of the Antarctic Margin*, 68 pp., 22 plates, AGU, Washington, D. C.

Bamber, J. L., R. E. M. Riva, B. L. A. Vermeersen, and A. M. LeBrocq (2009), Reassessment of the potential sea-level rise from a collapse of the West Antarctic Ice Sheet, *Science*, *324*, 901–903, doi:10.1126/science.1169335.

Barker, P. F., A. Camerlenghi, G. D. Acton, and A. T. S. Ramsay (2002), *Proc. Ocean Drill. Program Sci. Results*, vol. 178, pp. 1–40, Ocean Drill. Program, College Station, Tex. [Available at http://www-odp.tamu.edu/publications/178_SRN.]

Brancolini, G., and G. Leitchenkov (2010), Ross Sea, 118–128, in Cooper, A. K., G. Brancolini, C. Escutia, Y. Kristoffersen, R. Larter, G. Leitchenkov, P. O'Brien, and W. Jokat (2009), Chapter 5—Cenozoic climate history from seismic reflection and drilling studies on the Antarctic continental margin, in Developments in Earth and Environmental Sc*iences, Antarct*. Clim. Evol., vol. 8, edited by F. Florindo and M. Siegert, pp. 115–228, Elsevier, Netherlands, ISBN: 978-0-444-52847-6.

Brancolini, G., A. K. Cooper, and F. Coren (1995), Seismic facies and glacial history in the Western Ross Sea (Antarctica), *Ant. Res. Ser.*, 68 pp., 209–234, AGU, Washington, D. C.

Carlson, R. L., A. F. Gangi, and K. R. Snow (1986), Empirical reflection travel time versus depth and velocity versus depth functions for the deep-sea sediment column, *J. Geophy. Res.*, *91*(B8), 8249–8266, doi:10.1029/JB091iB08p08249.

Cooper, A. K., P. J. Barrett, K. Hinz, V. Traube, G. Leitchenkov, and H. M. J. Stagg (1991), Cenozoic prograding sequences of the Antarctic continental margin: A record of glacio-eustatic and tectonic events, *Mar. Geol.*, *102*, 175–213, doi:10.1016/0025-3227(91)90008-R.

Davey, F. J. (1987), Geology and structure of the Ross Sea region, in *The Antarctic Continental Margin: Geology and Geophysics of the Western Ross Sea. Circum-Pacific Council for Energy and Mineral Resources*, vol. 5B, edited by A. K. Cooper and F. J. Davey, pp. 1–16, CPCEMR Earth Sci. Ser., Houston, Tex.

Davey, F. J., and L. De Santis (2006), A multi-phase rifting model for the Victoria Land Basin, Western Ross Sea, *Antarctica, Contribution to Global Earth Sciences*, edited by D. K. Fütterer, pp. 303–308, Springer, Berlin, doi:10.1007/3-540-32934-X_38.

De Conto, R. M., and D. Pollard (2003), A coupled climate-ice sheet modeling approach to the Early Cenozoic history of the Antarctic ice sheet, *Palaeogeogr. Palaeoclimatol. Palaeoecol.*, *198*, 39–52, doi:10.1016/S0031-0182[03]00393-6.

De Santis, L., S. Prato, G. Brancolini, M. Lovo, and L. Torelli (1999), The Eastern Ross Sea continental shelf during the Cenozoic: Implications for the West Antarctic ice sheet development. *Global Planet. Change*, *23*, 173–196. PII:s0921-8181[99]00056-9.

De Santis, L., G. Brancolini, and F. Donda (2003), Seismo-stratigraphic analysis of the Wilkes Land continental margin (East Antarctica): Influence of glacially driven processes on the Cenozoic deposition, *Deep Sea Res., Part II*, *50*(8–9), 1563–1594, doi:10.1016/S0967-0645[03]00079-1.

Divins, D. L. (2003), *Total Sediment Thickness of the World's Oceans & Marginal Seas*, NOAA Natl. Geophys. Data Cent., Boulder, Colo. [Available at http://www.ngdc.noaa.gov/mgg/sedthick/.]

Eagles, G., K. Gohl, and R. D. Larter (2004), High-resolution animated tectonic reconstruction of the South Pacific and West Antarctic margin, *Geochem. Geophys. Geosyst.*, *5*, Q07002, doi:10.1029/2003GC000657.

Escutia, C., H. Brinkhuis, A. Klaus, and the Expedition 318 Scientists (2011), *Proceedings IODP, 318*, 101 pp., Integr. Ocean Drill. Program Manage. Int., Inc., Tokyo, doi:10.2204/iodp.proc.318.2011. [Available at http://publications.iodp.org/proceedings/318/104/104_.htm.]

Gohl, K. (2010), The Expedition of the research vessel "Polarstern" to the Amundsen Sea, Antarctica, in 2010 (ANT-XXVI/3), *Ber. Pol. Meeresforsch./Rep. Pol. Mar. Res.*, *617*, 173 pp., Alfred Wgener Institute Helmholtz Centre for Polar and Marine Research, Bremerhaven, Germany. [Available at http://epic.awi.de/29635/.]

Gohl, K., et al. (2007), Geophysical survey reveals tectonic structures in the Amundsen Sea embayment, West Antarctica, in *Antarctica: A Keystone in a Changing World—Online Proceedings of the 10th ISAES*, *USGS Open-File Rep. 2007-1047*, *Short Res. Pap. 047*, edited by A. K. Cooper and C. R. Raymond et al., 4 pp., doi:10.3133/of2007-1047.srp047.

Gohl, K., G. Uenzelmann-Neben, R. D. Larter, C.-D. Hillenbrand, K. Hochmuth, T. Kalberg, E. Weigelt, B. Davy, G. Kuhn and F. O. Nitsche (2013), Seismic stratigraphic record of the Amundsen Sea Embayment shelf from pre-glacial to recent times: Evidence for a dynamic West Antarctic Ice Sheet, *Mar. Geol.*, *344*, 115–131, doi:10.1016/j.margeo.2013.06.011.

Hayes, D. E., L. A. Frakes, and Shipboard_Scientific_Party (1975), A geophysical study of the Ross Sea, Antarctica Sites 270, 271, 272, in *Initial Reports of the Deep Sea Drilling Project, Leg 28*, edited by D. E. Hayes and L. A. Frakes, pp. 211–334, 887–907, U.S. Gov. Print. Off., Washington, D. C.

Hollister, C. D., et al. (Eds.) (1976), *Initial Reports of the Deep Sea Drilling Project*, vol. 35, U.S. Gov. Print. Off., Washington, D. C., doi:10.2973/dsdp.proc.35.1976.

Huang, X., K. Gohl, and W. Jokat (2014), Variability in Cenozoic sedimentation and paleo-water depths of the Weddell Sea basin related to pre-glacial and glacial conditions of Antarctica, *Global Planet. Change*, *118*, 25–41, doi:10.1016/j.gloplacha.2014.03.010.

Kalberg, T., and K. Gohl (2014), The crustal structure and tectonic development of the continental margin of the Amundsen Sea Embayment, West Antarctica: Implications from geophysical data, *Geophys. J. Int.*, *198*, 327–341, doi:10.1093/gji/ggu118.

Lear, C. H., T. R. Bailey, P. N. Pearson, H. K. Coxall, and Y. Rosenthal (2008), Cooling and ice growth across the Eocene-Oligocene transition, *Geology*, *36*, 251–254, doi:10.1130/G24584A.1.

Lindeque, A., Y. M. Martin, K. Gohl, and M. Maldonado (2013), Deep-sea pre-glacial to glacial sedimentation in the Weddell Sea and southern Scotia Sea from a cross-basin seismic transect, *Mar. Geol.*, *336*, 61–83, doi:10.1016/j.margeo.2012.11.004.

Lindeque, A., K. Gohl, S. Henrys, F. Wobbe, and B. Davy (2016), Seismic stratigraphy along the Amundsen Sea to Ross Sea continental rise: A cross-regional record of pre-glacial to glacial processes of the West Antarctic margin, *Palaeogeogr. Palaeoclimatol. Palaeoecol.*, *443*, 183–202, doi:10.1016/j.palaeo.2015.11.017.

Miller, K. G., J. D. Wright, M. E. Katz, J. V. Browning, B. S. Cramer, B.S. Wade, and S. F. (2008), A view of Antarctic ice-sheet evolution from sea-level and deep-sea isotope changes during the Late Cretaceous-Cenozoic, in *Proceedings of the 10th International Symposium on Antarctic Earth Sciences. Antarctica: A Keystone in a Changing World*, edited by A. K. Cooper et al., Natl. Acad. Press, Washington, D. C., doi:10.3133/of2007-1047.kp06.

Müller, R.D., K. Gohl, S. C. Cande, A. Goncharov, and A. V. Golynsky (2007), Eocene to Miocene geometry of the West Antarctic rift system. *Aust. J. Earth Sci.*, *54*, 1033–1045, doi:10.1080/08120090701615691.

Nitsche, F. O., K. Gohl, K. Vanneste, and H. Miller (1997), Seismic expression of glacially deposited sequences in the Bellingshausen and Amundsen Seas, West Antarctica, in *Geology and Seismic Stratigraphy of the Antarctic Margin 2*, vol. 71, edited by P. F. Barker and A. K. Cooper, *Antarct. Res. Ser.*, pp. 95–108, AGU, Washington, D. C.

Nitsche, F. O., A. P. Cunningham, R. D. Larter, and K. Gohl (2000), Geometry and development of glacial continental margin depositional systems in the Bellingshausen Sea, *Mar. Geol.*, *162*(2–4), 277–302.

Rebesco, M., R. D. Larter, P. F. Barker, A. Camerlenghi, and L. E. Vanneste (1997), The history of sedimentation on the continental rise west of the Antarctic Peninsula, in *Geology and Seismic Stratigraphy of the Antarctic Margin 2, Antarctic Res. Ser.*, edited by P. F. Barker and A. K. Cooper, 71, 29–49, AGU, Washington, D. C.

Scheuer, C., K. Gohl, and G. Eagles (2006), Gridded isopach maps from the South Pacific and their use in interpreting the sedimentation history of the West Antarctic continental margin. *Geochem. Geophys. Geosyst.*, *7*, Q11015, doi:10.1029/2006GC001315.

Smith, R. T., and J. B. Anderson (2010), Ice-sheet evolution in James Ross basin, Weddell Sea margin of the Antarctic Peninsula: The seismic stratigraphic record, *Geol. Soc. Am. Bull.*, *122*(5/6), 830–842, doi:10.1130/B26486.1.

Smith, R. T., and J. B. Anderson (2011), Seismic stratigraphy of the Joinville Plateau: Implications for regional climate evolution, in *Tectonic, Climatic, and Cryospheric Evolution of the Antarctic Peninsula*, edited by J. B. Anderson and J. S. Wellner, pp. 51–61, Geopress, AGU, Washington, D. C., doi:10.1029/2010SP000980.

Smith, W. H. F., and P. Wessel (1990), Gridding with continuous curvature splines in tension, *Geophysics*, *55*, 293–305.

Tucholke, B. E., N. T. Edgar, and R. E. Boyce (1976), Physical properties of sediments and correlations with acoustic stratigraphy: Leg 35, Deep Sea Drilling Project, in *Initial Reports*, edited by C. D. Hollister and C. Craddock, pp. 229–249, Deep Sea Drill. Proj., Washington, D. C.

Uenzelmann-Neben, G. (2006), Depositional patterns at Drift 7, Antarctic Peninsula: Along-slope versus down-slope sediment transport as indicators for oceanic currents and climatic conditions, *Mar. Geol.*, *233*(1–4), 49–62, doi:10.1016/j.margeo.2006.08.008.

Uenzelmann-Neben, G., and K. Gohl (2012), Amundsen Sea sediment drifts: Archives of modifications in oceanographic and climatic conditions. *Mar. Geol.*, *299–302*, 51–62, doi:10.1016/j.margeo.2011.12.007/.

Uenzelmann-Neben, G., and K. Gohl (2014), Early glaciation already during the Early Miocene in the Amundsen Sea, Southern Pacific: Indications from the distribution of sedimentary sequences, *Global Planet Change*, *120*, 92–104, doi:10.1016/j.gloplacha.2014.06.004.

Wessel, P., W. H. F. Smith, R. Scharroo, J. Luis, and F. Wobbe (2013), Generic mapping tools: Improved version released, *EOS Trans. AGU*, *94*(45), 409–410, doi:10.1002/2013EO450001.

Whittaker, J., A. Goncharov, S. Williams, R. D. Müller, and G. Leitchenkov (2013), Global sediment thickness data set updated for the Australian-Antarctic Southern Ocean, *Geochem. Geophys. Geosyst.*, *14*, 3297–3305, doi:10.1002/ggge.2018.

Wilson, D. S., and B. Luyendyk (2009), West Antarctic paleotopography estimated at the Eocene-Oligocene climate transition, *Geophys. Res. Lett.*, *36*, L16302, doi:10.1029/2009GL039297.

Wilson, D. S., S. S. R. Jamieson, P. J. Barrett, G. Leitchenkov, K, Gohl, and R. D. Larter (2012), Antarctic topography at the Eocene-Oligocene boundary, *Palaeogeogr., Palaeoclimatol. Palaeoecol.*, *335–336*, 24–34, doi:10.1016/j.palaeo.2011.05.028.

Wilson, D. S., D. Pollard, R. M. DeConto, S. S. R. Jamieson, and B. P. Luyendyk (2013), Initiation of the West Antarctic Ice Sheet and estimates of total Antarctic ice volume in the earliest Oligocene, *Geophys. Res. Lett.*, *40*, 4305–4309, doi:10.1002/grl.50797.

Wobbe, F., K. Gohl, A. Chambord, and R. Sutherland (2012), Structure and breakup history of the rifted margin of West Antarctica in relation to Cretaceous separation from Zealandia and Bellingshausen plate motion, *Geochem. Geophys. Geosyst.*, *13*, Q04W12, doi:10.1029/2011GC003742.

Wobbe, F., A. Lindeque, and K. Gohl (2014), Anomalous South Pacific lithosphere dynamics derived from new total sediment thickness estimates off the West Antarctic margin, *Global Planet. Change*, *123*, 139–149, doi:10.1016/j.gloplacha.2014.09.006.

Yamaguchi, K., Y. Tamura, I. Mizukoshi, and T. Tsuru (1988), Preliminary report of geophysical and geological surveys in the Amundsen Sea, West Antarctica, *Proc. NIPR Symp. Antarct. Geosci.*, *2*, 55–67.

Zachos, J., M. Pagani, L. Sloan, E. Thomas, and K. Billups (2001), Trends, rhythms, and aberrations in global climate 65 Ma to present, *Science*, *292*, 686–693.

Zachos, J. C., G. R. Dickens, and R. E. Zeebe (2008), An early Cenozoic perspective on greenhouse warming and carbon-cycle dynamics, *Nature*, *451*, 279–283, doi:10.1038/nature06588.

Zwally, H. J., M. B. Giovinetto, M. A. Beckley, and J. L. Saba (2012), *Antarctic and Greenland Drainage Systems*, GSFC Cryosp. Sci. Lab., United States National Space Agency (NASA). [Available at http://icesat4.gsfc.nasa.gov/cryo_data/ant_grn_drainage_systems.php.]